CHAPTER V
PREPARATION OF POLY(VINYL ALCOHOL)/TIN GLYCOLATE COMPOSITE FIBERS BY COMBINED SOL-GEL/ELECTROSPINNING TECHNIQUES AND THEIR CONVERSION TO ULTRAFINE TIN OXIDE FIBERS

5.1 Abstract

Ultra-fine composite fibers made from poly(vinyl alcohol) (PVA)/tin glycolate — a moisture stable tin oxide containing compound — were prepared by a combined sol–gel processing and electrospinning technique. These fibers were subsequently converted to ultrafine tin oxide fibers by calcination treatment, with the aim of producing tin oxide fiber with a high surface area-to mass ratio and a high specific conductivity value. The acidity of spinning solution plays an important role to the morphology and size of the obtained fibers. The average diameters of the obtained composite fibers were in the range of 87-166 nm. It was found that the ultrafine tin oxide fiber showed the high conductivity value of 1.59 $x10^3$ Scm^{-1} at calcinations temperature of 600°C, and the BET surface area was in a range of 71 and 275 m^2/g. Moreover, the effect of calcinations temperature on the phase and the size of the tin oxide fibers were investigated in this study.

(**Keywords**: Electrospinning; Tin oxide fibers; Tin Glycolate)

5.2 Introduction

Tin oxide (SnO_2) in its pure tetragonal rutile crystal structure (e.g., cassiterite mineral) exhibits the n-type semiconducting character with a wide direct energy band gap of 4 eV and an indirect band gap of 2.6 eV [1]. It is recognized as one of the key functional metal-oxide semiconductors (MOS) owing to its excellent chemical and electrical properties. Therefore, SnO_2 is widely used in optoelectronic devices [2], gas sensors for detecting leakage, flat panel displays [3], and as catalyst supports. The important factor for high sensing performance is high surface-area-to-

volume ratio [4-7], and electrospinning (e-spinning) technique is the one that satisfies this need since the key advantages of this technique are unique, cost-effective route, and providing high surface area to volume ratio on fibers, when compared with those of the corresponding films [8,9]. Moreover, the e spinning process can be applied to materials of diverse origins, such as natural or synthetic polymers as well as sol-gel-based ceramics. The sol-gel process itself has many advantages over other techniques, some of which are homogeneity, stoichiometric control and purity of the products as well as the simplicity of the process [1]. Recently, some inorganic fibers have been successfully prepared by the combined sol-gel processing and e-spinning technique [8-10].

Dharmaraj *et al.* [11] prepared SnO_2 fibers (100-150 nm in diameters) from the e-spun tin/poly(vinyl acetate) (PVAc) composite fibers after calcinations at 300–600 °C. The sol suspension was prepared from $SnCl_2{\cdot}2H_2O$ and PVAc (14 wt%) in the 1:0.8 weight ratios. Shukla *et al.* [12] prepared SnO_2 fibers (45-280 nm in diameters) using the elctrospun hydroxypropyl cellulose (HPC) fibers as templates. For this purpose, the sol suspension was mixed between HPC and $SnCl_2{\cdot}2H_2O$ in a weight ratio of 1.75:1. Zhang *et al.* [13] also prepared SnO_2 fibers (~100 nm in average diameters) obtained by e-spinning of a poly(vinyl alcohol) (PVA)/$SnCl_4{\cdot}5H_2O$ solution with 6 % PVA after annealing at 700°C. These fibers were also used as a novel gas sensing material.

It is evident that all of 1 these previous reports utilized $SnCl_2{\cdot}2H_2O$ or $SnCl_4{\cdot}5H_2O$ as the source of tin and illustrated fairly small surface-area-to-volume-ratio, though their sensing characteristic was good. Therefore, our aim is to explore the use of a novel material, moisture stable tin glycolate, directly synthesized from tin oxide and ethylene glycol [14], as the tin source for fabrication of e-spun SnO_2 fibers, using PVA as the polymer gelator. Moreover, another key goal is to prepare high surface area SnO_2 fibers by the combined sol-gel processing and e spinning technique for high sensitivity in sensing devices. In the present work the obtained composite fibers were subsequently converted into ultrafine SnO_2 fibers by calcinations. The obtained fibers were then characterized for their chemical integrity, crystal structure, surface area, and finally, conductivity.

5.3 Experimental Section

5.3.1 Preparation of Tin Glycolate

The method for the preparation of tin glycolate was described previously [14]. Briefly, a mixture of 15 g of tin (IV) oxide (0.1 mol; 99% purity; Sigma-Aldrich, USA) and 14.6 g of triethylenetetramine (TETA, 0.03 mol; 98% purity; Facai Polytech Co., Ltd, Thailand) was stirred vigorously in an excess amount of ethylene glycol (EG, 100 mL; 100% purity; Merck, USA) and heated to 200°C for 24 h. The resulting solution was placed *in vacuo* to remove unreacted EG, resulting in a crude precipitate. The crude white solid product was then washed with acetonitrile (99% purity; Labscan (Asia), Thailand), dried in a vacuum desiccator, and characterized using fourier-transformed infrared spectroscopy (FT-IR) and thermo gravimetric analysis (TGA).

FT-IR: 2930–2830 cm^{-1} (υC-H), 1077 cm^{-1} (υC-O), 900–880 cm^{-1} (υSn-O-C) and 600–550 cm^{-1} (υSn-O); TGA: 63.2% ash yield.

5.3.2 Electrospinning of PVA/Tin Glycolate Solutions and Preparation of SnO_2 Fibers

PVA/tin glycolate solution was first prepared by mixing 0.04 g of tin glycolate with 20 μL of 8 M HNO_3 and 200 μL of water. It should be noted that only in the case where the effect of the acid type was investigated the type of the acid was changed to either 8 M CH_3COOH or 8 M HCl. The solution was then added into 5 mL of an aqueous PVA solution (M_w = 72,000 Da and degree of hydrolysis ≥ 98%; Sigma-Aldrich, USA). The concentration of the base PVA solution was varied between 6 and 13 wt% and the resulting mixture was constantly stirred for 5 min. The as-prepared solutions were referred to as the spinning solutions.

A schematic drawing of the e-spinning setup utilized in this work can be found elsewhere [10]. Specifically, each of the spinning solutions was loaded into a plastic syringe. A blunt 20-gauge stainless-steel hypodermic needle was used as a nozzle. Both the syringe and the nozzle were tilted ~45° from a horizontal baseline to maintain a constant presence of a droplet at the tip of the nozzle. A Gamma High Voltage Research UC5-30P dc power supply was used to charge the spinning solution by connecting the emitting electrode (positive) to the nozzle and the

grounding one to an aluminum sheet wrapped around a rigid plastic backing, used as a collection device. The distance between the tip of the nozzle and the collection device defines a collection distance. For the preparation of the PVA/tin glycolate composite fibers, the following parameters were varied to investigate their effects on the morphological appearance of the obtained fibers: the concentration of the spinning solutions (i.e., 6-13 wt% of the base PVA solutions under a fixed electric field of 15 kV/10 cm), the type of acid [i.e.,CH_3COOH (pK_a = 4.76), HNO_3 (pK_a = -1.4) or HCl (pK_a = -7) for the spinning solution from a base PVA solution of 10 wt% under a fixed electric field of 12.5 kV/15 cm], the applied electrical potential (i.e., 10-15 kV over a fixed collection distance of 15 cm for the spinning solution from a base PVA solution of 10 wt%), and the collection distance (i.e., 8–15 cm for the spinning solution from a base PVA solution of 10 wt% and a fixed applied potential of 12.5 kV). For these studies, the collection time was fixed at ~5 min and all experiments were done in climate control room at 25 °C which had relative humidity 55 ± 2%. The PVA/tin glycolate composite fibers that had been prepared from a spinning solution with a concentration of the base PVA solution of 10 wt% and 8M HNO_3 under a fixed electric field of 12.5 kV/15 cm were used to further investigate the effect of calcination temperature on the morphological appearance, properties and structures of the post-calcined SnO_2 fibers. The e-spun fibers had been exposed to ambient moisture (about 55 ± 2% RH) for ~5 h before being calcined in a Carbolite CFS 1200 furnace over a temperature range of 400 to 1000°C for ~5 h. The heating program started from room temperature to each specified calcinations temperature at a heating rate of 0.5°C min^{-1}.

5.3.3 Characterization

The morphological appearance and the diameters of the e-spun PVA/tin glycolate composite fibers and the as-calcined SnO_2 fibers were observed by a JEOL 5200-2AE scanning electron microscope (SEM). The diameters of the obtained fibers were measured directly from SEM images, using SEMAphore 4.0 software, from which the average values were calculated ($n \geq 100$). TGA was carried out on a Perkin-Elmer Pyris Diamond TG/DTA over a temperature range of 30-900°C at a heating rate of 10°C min^{-1} under nitrogen atmosphere. Chemical integrity

of the materials was observed on a Nicolet Nexus 670 FT-IR spectroscope over the wavenumber range of 400–2500 cm^{-1} at a resolution of 4 cm^{-1} using the KBr pellet method. The microstructure of the as-calcined SnO_2 fibers was investigated by wide-angle X-ray diffraction (WAXD) on a Rigaku D/MAX-2000 X-ray diffractometer using CuKα over a scanning range of 20–70° with at a scanning speed of 5° min^{-1} and a 0.02 scanning step. The Brunauer-Emmett-Teller (BET) surface area of both the pre- and the post-calcined fibers was measured using a Quantachrome Quantasorb JR Autosorp-1 gas sorption system (Quantachrome, Boynton Beach, FL). All of the samples were degassed at 300°C prior to the before measurements. The electrical conductivity values of the as-calcined SnO_2 ultrafine tin oxide fibers were measured by a custom-built two-point probe with copper as electrodes, coupled to a Keithley 6517A voltmeter (Keithley, Model 6517A). The current used was in the linear Ohmic regime.

5.4 Results and Discussion

5.4.1 Electrospun PVA/Tin Glycolate Composite Fibers

To investigate the effect of the PVA concentration on the morphological appearance of the obtained composite fibers, the concentration of the base PVA solutions was varied at 6, 10 and 13 wt%. The as-prepared PVA/tin glycolate solutions were spun at a fixed electric field of 15 kV/10 cm. Figure 5.1 shows representative SEM images of the obtained fibers. In general agreement with our previous work on the preparation of PVA/silatrane composite fibers by e spinning [10], a combination of smooth and beaded fibers was obtained when the concentration of the base PVA solution was 6 wt%. The formation of beads was due to the dominating effect of the surface tension that was responsible for the capillary instability of the charged jet [1]. At this condition, the diameters of the obtained fibers were 162 ± 100 nm. Despite the fact that only the fiber segments between beads were measured for the diameters, the large deviation in the diameters of the fibers was obviously resulting from the presence of the beads.

When the concentration of the base PVA solution increased to 10 and 13 wt%, only smooth fibers were the dominant features. The diameters of these

fibers were 158 ± 43 and 375 ± 100 nm, respectively. The increase in the chain entanglements in response to the increase in the concentration, hence the viscosity of the base PVA solution was the obvious reason for the observed increase in the diameters of the obtained fibers [1, 15]. At a high concentration, the viscosity of the spinning solution could be too great, which could lead to non-uniform flow of the liquid through the opening of the nozzle, resulting in the non uniform ejection of the jet. The non-uniform ejection could finally lead to the formation of fibers with uneven diameters and this is the likely explanation for the obviously large deviation in the diameters of the fibers obtained from the spinning solution that had been prepared from the 13 wt% PVA solution.

Next, we investigated the effect of the type of acid on the morphological appearance of the composite fibers obtained from the spinning solution that had been prepared from the 10 wt% PVA solution under a fixed electric field of 12.5 kV/15 cm. Representative SEM images of the obtained fibers are shown in Figure 5.2. The fibers that were obtained from the spinning solution that had been prepared without the addition of acid (i.e., the water system) were used as the controlled condition. The results clearly showed that the acidity of the spinning solution played an important role in determining the morphology of the obtained fibers. Specifically, for the water system, a combination of smooth and beaded fibers was obtained. The number of beaded fibers was found to decrease with an increase in the acidity of the spinning solution, i.e., for the spinning solution containing CH_3COOH. For the spinning solution containing a stronger acid, i.e., HNO_3, predominantly smooth fibers were obtained. Further increasing the acidity of the spinning solution, especially, for the one containing HCl, beaded fibers reappeared. Such a variation in the acidity, also implying the pH and the total number of ionic species, of the spinning solution influenced the sol-gel reaction of the tin glycolate, the viscosity of the solution, the conductivity of the solution, and thus, the electrical forces acting on the ejected jet.

The effect of the applied electrical potential on the morphology of the obtained fibers was the next to be investigated. Here, the electrical potential in the range of 10 to 15 kV was applied to the spinning solution that had been prepared from the 10 wt% PVA solution and 8M HNO_3 over a fixed collection distance of 15

cm. Representative SEM images of the obtained fibers are shown in Figure 5.3. While only the fibers that was obtained at the applied electrical potential of 12.5 kV were smooth, a combination of smooth and beaded fibers were obtained when applied electrical potential was either 10 or 15 kV. At a given collection distance, an increase in the applied electrical potential used to charge the spinning solution generally resulted in the observed decrease in both the number and the size of the beads. The increase in the applied electrical potential was responsible for the increase in the electrical forces imposed on a droplet of the spinning solution at the tip of the nozzle as well as the subsequent, ejected jet [15,16]. Moreover, the increase in the applied electrical potential could also result in an increase in the electrostatic force, causing the diameters of e-spun fibers to increase. The increases in both the speed of the jet segment and the mass flow rate, in turn cause the onset of the bending instability to occur closer to the collection device [15,16]. Without a strict control over the flow rate of the spinning solution through the nozzle, the size of the pendant droplet could grow over time, despite a constant ejection of the jet from the apex of the droplet cone. The ejection of the overgrown droplet could present either as a discrete droplet or as a part of the jet, which for the latter, under the action of the electrical forces, would become elongated, and this could be the reason for the reappearance of the beaded fibers when the applied electrical potential increased from 12.5 to 15 kV.

The effect of the collection distance on the morphology of the obtained fibers was the next to be investigated. Here, the electrical potential of 12.5 kV was applied to the spinning solution that had been prepared from the 10 wt% PVA solution and 8M HNO_3 over a collection distance range of 8 to 15 cm. Representative SEM images of the obtained fibers are shown in Figure 5.4. Evidently, a combination of smooth and beaded fibers was observed at the shortest collection distance studied (i.e., at 8 cm). The number of the beaded fibers decreased sharply as the collection distance increased to 10 cm, with only the smooth fibers being the dominant feature at the highest collection distance studied (i.e., at 15 cm). The likelihood for the formation of beaded fibers at the shortest collection distance investigated (i.e., 8 cm) should be attributed to the short time as well as the short path distance that the ejected jet traveled to the collector in response to the greatest

electrical forces exerting on it. Such a short time and a short distance may not be enough for the beads, if being present, to be fully elongated prior to the deposition on the collector. As the collection distance increased further, despite the consistently lower electrical forces acting on the jet, the longer time and the longer distance for the traveling jet should be the reason for the fully stretching of the beads to finally obtain the smooth fibers on the collector. With regards to the size of the obtained fibers, it is evident that the diameters decreased monotonically from 227 ± 85 to 147 ± 33 nm as increasing the collection distance from 8 to 15 cm, respectively.

5.4.2 Preparation of Tin Oxide Fibers

5.4.2.1 Effect of type of acid on composite fiber after calcinations

From the previous effect, it was found that type of acid plays an important role on the morphology of PVA/tin glycolate composite fibers. Next, the composite fibers obtained from the spinning solution that has been prepared from the 10 wt% PVA solution under the applied electric field of 12.5 kV/15 cm were chosen to further investigate the effect of type of acid (i.e., 8M CH_3COOH, 8M HCl, and 8M HNO_3) on morphology after calcination at 600°C. Representative SEM images of the obtained fibers are shown in Figure 5.5. Upon calcination, both of the composite fibers obtained from the spinning solution that has been prepared from 8M CH_3COOH and 8M HCl provided bigger size of fibers, i.e., 1470 ± 88 nm, 1249 ± 41 nm, respectively, (see Figures 5.5 a and b) because many beads along fibers were fused together at high temperature. On the other hand, the fibrous nature of the original composite fibers was retained, but the as-calcined fibers prepared from the spinning solution containing 8M HNO_3 shrank considerably (see Figure 5c) because of the decomposition of the organic PVA content within the fibers [9]. The diameter of the as-calcined fibers decreases to 121 ± 26 nm.

5.4.2.2 Effect of calcinations temperature

Based on all of the spinning conditions investigated, the PVA/tin glycolate composite fibers that had been prepared from the spinning solution with the concentration of the base PVA solution of 10 wt% and 8M HNO_3 under the applied electric field of 12.5 kV/15 cm were chosen to further investigate the effect of the calcination temperature on morphology, structure and properties of the post-calcined fibers. The calcination temperature was varied between 400 and

1000°C. Figure 5.6 shows representative SEM images of the neat PVA/tin glycolate composite fibers as well as the post-calcined products. As previously described, the neat composite fibers that had been prepared from the chosen spinning condition were smooth, with the diameters being 172 ± 21 nm. After calcination, the shrinkage of the fibers along both the fiber and the radial directions was evident, with the extent of such shrinkage becoming more pronounced with an increase in the calcination temperature. Specifically, the diameters of the as-calcined fibers decreased to 166 ± 46 nm at the calcination temperature of 400°C, which continued to decrease to 87 ± 18 nm at 1000°C.

The chemical integrities of the neat PVA/tin glycolate composite fibers and the post calcined products were further investigated by FT-IR, as graphically shown in Figure 7. According to the FT-IR spectrum of the neat composite fibers, the absorption peaks at 1440 cm^{-1} (CH_2 bending) and 858 cm^{-1} (CH_2 rocking) characteristic to PVA [17] were evident. These peaks were, however, absent from the spectra of the as-calcined products, indicating the complete removal of the PVA template. It was shown that according to the TGA result with a heat scanning rate of 10 °Cmin^{-1} under a nitrogen atmosphere PVA in the form of solvent-cast films lost about 80% of its mass when the temperature reached 400°C [17]. As shown in Figure 5.7, a new absorption peak centering around 600–630 cm^{-1}, characteristic to the vibration of Sn-O bond, was observed in all of the FT-IR spectra of the as-calcined products. Clearly, the intensity of this peak for the products was much more pronounced as increasing the calcinations temperature. As a conclusion, the PVA/tin glycolate composite fibers were successfully transformed into SnO_2 fibers.

WAXD was used to further investigate the microstructure of the post-calcined products and the results are shown in Figure 5.8. All of the WAXD patterns indicated that the as-calcined products were crystalline in nature. All of the fibers that had been calcined at the calcination temperatures of 400, 600, and 800°C showed the diffraction peaks characteristic to the tetragonal rutile SnO_2 crystals. At 1000°C, the peaks were much more pronounced with additional peaks being observed. According to the JCPDS card No. 21-1250, the positions of these peaks indicated that the SnO_2 crystals in the obtained fibers existed in the pure tetragonal

rutile phase as in the cassiterite mineral. Moreover, the crystallite size of all the post-calcined products are evaluated from the FWHM of the XRD reflections using Scherer's equation [18]; in which $D = K(\lambda/\beta \cos \theta)$ where $K = 0.89$ (constant), $\lambda = 0.154$ nm (X-ray wavelength) of Cu-Kα radiation), β = the full width of half maximum for the diffraction peak and θ = scattering angle. In the present work, the average crystallite size of the SnO_2 is calculated from SnO_2 (101) reflection peak from the XRD pattern. The values of the calcined tin oxide fibers at 400, 600, 800, and 1000°C were 3.91, 5.38, 9.49, and 82.53, nm respectively. The results clearly showed that both the extent and the size of the crystals increased with an increase in the calcination temperature [7,19-22]. The BET surface area of both the neat PVA/tin glycolate composite fibers and the post-calcined fibers was also determined. The surface area of the composite fibers was determined to be about 17 m^2g^{-1}, while those of the as-calcined fibers at 400 and 600°C were about 121 and 275 m^2g^{-1} due to the presence of PVA in the neat PVA/tin glycolate composite fibers not completely decomposed at this temperature [9]. However, as calcinations temperatures increased higher to 800 and 1000°C, as-calcined fibers were found to exhibit a decrease in the surface areas to 186 and 71 m^2g^{-1}, respectively. The monotonous decrease in the BET surface area of the SnO_2 fibers with an increase in the calcination temperature was obviously a result of the observed increase in the hypothetical increase in the size of the cassiterite crystals.

As a semiconducting material, the specific conductivity of the post-calcined fibers is of great interest. The results of the measurements are summarized in Table 5.1, along with those of the neat PVA/tin glycolate composite fibers and the tin glycolate precursor itself. Clearly, all of the as-calcined fibers exhibited the property values in the range of 3.46×10^2 to 1.59×10^3 Scm^{-1} on average, with the value for the fibers that had been calcined at 600 °C being the greatest. These values certainly fall within the semiconductor regime, indicating that these ultrafine SnO_2 fibers have a high potential for use as a 2D semiconductor. Interestingly however, the specific conductivity values reported here for these fibers were much greater than those generally reported for the conventional SnO_2 films (i.e., 10^1 - 10^2 Scm^{-1}) [23-25]. In addition, the decrease in the conductivity value should be

a result of the observed decrease in the surface area of the crystals as increasing the calcination temperatures [26]. Comparatively, such values for the neat PVA/tin glycolate composite fibers and the tin glycolate precursor were much lower at 4.82×10^{-2} and 2.24×10^{-1} Scm^{-1}, respectively, on average.

5.5 Conclusions

Ultrafine tin oxide fibers with diameters in the range of 87–166 nm have been successfully prepared by calcining the sol-gel derived electrospun PVA/tin glycolate composite fibers (based on the e-spinning of PVA (10 wt%)/tin glycolate — moisture stable tin containing-compound — solution under the applied electric field of 12.5 kV/15 cm). The diameters of the composite fibers increased with an increase in the concentration of the base PVA solution. The acidity of the solvent plays an important role to the morphology of fibers. HNO_3 is not only a good candidate to be a catalyst for the sol-gel processing of tin glycolate, but also provides small size of SnO_2 fibers after calcination. The applied electrical potential has significant impact to the size and the surface morphology of the fiber. The fiber diameter and the bead formation were decreased with increasing collection distance. The average diameter of the post calcined fibers decreases from 166 ± 46 nm to 87 ± 18 nm with increasing the calcinations temperature from 400 to 1000°C, respectively. The FT-IR results confirmed the presence of the Sn-O bond of the tin oxide fiber, as well as the WAXD, postulating the tetragonal rutile tin oxide fiber. Moreover, raising the heat treatment temperature from 600 to 1000°C causes the decrease in surface areas and specific conductivity. The ultrafine tin oxide fiber showed the high conductivity value of 1.59×10^{3} Scm^{-1} and the highest BET surface area of 275 m^2/g at the 600°C calcinations temperature.

5.6 Acknowledgements

This research work was supported by (1) The National Center for Petroleum, Petrochemicals and Advanced Materials (C-PPAM), Chulalongkorn University, (2)

The Ratchadapisake Sompote Fund, Chulalongkorn University, and (3) The Thailand Research Fund (TRF).

5.7 References

1. O. P. Agnihotri, M. T. Mohammad, A. K. Abass and K. I. Arshak, "Electrical and optical properties of chemically deposited conducting glass for SIS solar cells", *Solid State Commun*, **47**, 195-198 (1983).
2. C. Tatsuyama and S. Ichimura, "Electrical and Optical Properties of GaSe-SnO_2 Heterojunctions", *Jpn. J. Appl. Phys.*, **15**, 843-847 (1976).
3. Y. Matsui, Y. Yamamoto and S. Takeda, "Electron-Emissive Materials, Vacuum Microelectronics and Flat-Panel Displays, San Francisco, U.S.A., April 25–27, 2000, Materials Research Society Symposium Proceedings", **621**, Q.4.9.1. (2000).
4. N. V. Hieu, H. R. Kim, B. K. Ju, and J. H. Lee, "Enhanced performance of SnO_2 nanowires ethanol sensor by functionalizing with La_2O_3", *Sens. Actuators B Chem.*, **133** 228-234 (2008).
5. J. Hu, Y. Bando, Q. Liu, and D. Golberg, "Laser-ablation growth and optical properties of wide and long single-crystal SnO_2 ribbons", *Adv. Funct. Mater.*, **13**, 493-496 (2003).
6. Q. Kuang, C. Lao, Z. L. Wang, Z. Xie, and L. Zheng, "High-sensitivity humidity sensor based on a single SnO_2 nanowires", *J. Am. Chem. Soc.*, **129**, 6070-6071 (2007).
7. X. Y. Xue, Y. J. Chen, Y. G. Wang, and T. H. Wang, "Synthesis and ethanol sensing properties of $ZnSnO_3$ nanowires", Appl. Phys. Lett., **86**, 233101/1-2.
8. S. Li, C. Shao, Y. Lui, S. Tang, R. Mu, "Nanofibers and nanoplatelets of MoO_3 via an electrospinning technique", *Journal of Physics and Chemistry of Solids*, **67**, 1896 1872 (2006).
9. M. Krissanasaeranee, T. Vongsetskul, R. Rangkupan, P. Supaphol, and S. Wongkasemjit, "Preparation of Silica Nanofibers Using Electrospun Poly(vinyl alcohol)/Silatrane Composite Nanofibers as Precursor", *J. Am. Cer. Soc.*, **91 [9]**, 2830–2835 (2008).

10. N. Dharmaraj, H. C. Park, C. K. Kim, H. Y. Kim, D. R. Lee, "Nickel titanate nanofibers by electrospinning", *Materials Chemistry and Physics*, **87**, 5-9 (2004).
11. N. Dharmaraj, C. H. Kim, K. W. Kim, H. Y. Kim, and E. K. Suh, "Spectral studies of SnO_2 nanofibers prepared by electroapinning method", *Spect. Acta Part A*, **64**, 136-140 (2005).
12. S. Shukla, E. Brinley, H. J. Cho, and S. Seal, "Electroapinning of hydroxypropyl cellulose fibers and their application in synthesis of nano and submicron tin oxide fibers", *Polymer*, **46**, 12130-12145 (2005).
13. Y. Zhang, X. He, J. Li, Z. Miao, and F. Huang, "Fabrication and ethanol-sensing properties of micro gas sensor based on electrospun SnO_2 nanofibers", *Sens. And Actuators B*, **132**, 67-73(2008).
14. C. Junin, M. Krissanasaeranee, A. M. Jamieson, S. Wongkasemjit, "Synthesis of high surface area tin oxide via sol-gel process using tin glycolate precursor", *J. Sci.*, **32**, 385- 390 (2005).
15. C. Mit-uppatham, M. Nithitanakul, and P. Supaphol, "Ultrafine e*lectrospu*n polyamide-6 fibers: effect of solution conditions on morphology and average fiber diameter," *Macromol. Chem. Phys.*, **205**, 2327-2338 (2004).
16. P. Supaphol and S. Chuangchote, "On the electrospinning of poly(vinyl alcohol) nanofibers mats: a revisit," *J. Appl. Polym. Sci.*, **108**, 969-978 (2008).
17. J. Sriupayo, P. Supaphol, J. Blackwell, R. Rujiravanit, "Preparation and characterization of a-chitin whisker-reinforced poly(vinyl alcohol) nanocomposite films with or without heat treatment," *Polymer* **46**, 5637–5644 (2005).
18. B. D. Cullity, *Elements of X-ray Diffraction (2nd ed.)*. Addison-Wesley, 1978.
19. J. Q. Hu, Y. Bando, D. Golberg, "Self-catalyst growth and optical properties of novel SnO_2 fishbone-like nanoribbons" *Chem. Phys. Lett.* **372**, 758-762 (2003).
20. Y. He, Y. Li, J. Yu, Y. Qian, "Chemical control synthesis of nanocrystalline SnO_2 by hydrothermal reaction", *Mater. Lett.* **40**, 23-26 (1999).
21. F. Gu, S. F. Wang, C. F. Song, M. K. Lu, Y. X. Qi, G. J. Zhou, D. Xu, D. R. Yuan, "Synthesis and luminescence properties of SnO_2 nanoparticles", *Chem. Phys. Lett.* **372**, 451-454 (2003).

22. K. N. Yu, Y. H. Xiong, Y. L. Liu, C. S. Xiong, "Microstructural change of nano SnO_2 grain assemblages with annealing temperature", *Phys. Rev. B*, **55**, 2666-2671 (1997).
23. J. B. Han, H. J. Zhou, Q. Q. Wang, "Conductivity and optical nonlinearity of Sb doped SnO_2 films", *Materials Letters*, **60**, 252 – 254 (2006).
24. S. C. Ray, M. K. Karanjai, D. Dasgupta, "Tin dioxide based transparent semiconducting films deposited by the dip-coating technique", *Surface and Coatings Technology*, **102**, 73–80 (1998).
25. M. M. Bagheri-Mohagheghi, N. Shahtahmasebi, M. R. Alinejad, A. Youssefi, M. Shokooh-Saremi, "Fe-doped SnO_2 transparent semi-conducting thin films deposited by spray pyrolysis technique: Thermoelectric and p-type conductivity properties", *Solid State Sciences*, 1-7 (2008).
26. J. Zhang and L. Gao, "Synthesis and characterization of nanocrystalline tin oxide by sol gel method", *J. Solid State Chem.*, **177**, 1425-1430 (2004).

Table 5.1 The specific conductivity of tin glycolate, neat PVA/tin glycolate fibers and post-calcined fibers at different calcination temperatures.

Sample	The specific conductivity (S cm^{-1})
Tin glycolate	$2.24 \times 10^{-1} \pm 4.36 \times 10^{-5}$
Neat PVA/tin glycolate fibers	$4.82 \times 10^{-2} \pm 3.98 \times 10^{-4}$
Post-calcined fibers at 400°C	$5.67 \times 10^{-2} \pm 3.02 \times 10^{-4}$
Post-calcined fibers at 600°C	$1.59 \times 10^{-3} \pm 5.76 \times 10^{-5}$
Post-calcined fibers at 800°C	$8.05 \times 10^{-2} \pm 3.26 \times 10^{-4}$
Post-calcined fibers at 1000°C	$3.46 \times 10^{-2} \pm 2.97 \times 10^{-5}$

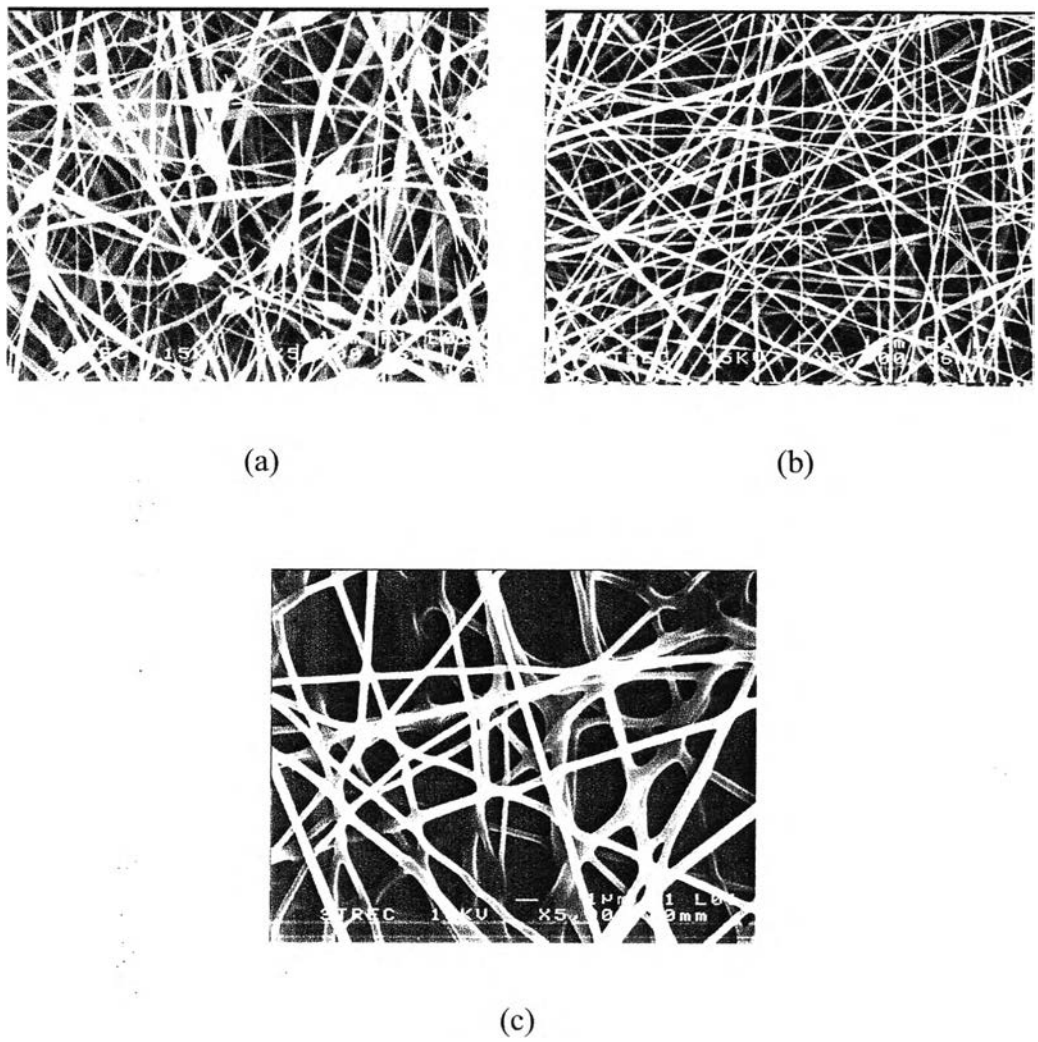

Figure 5.1 SEM images of pre-calcined as-spun fibers from spinning solutions containing (a) 6, (b) 10, and (c) 13 wt% PVA solution, using the applied electrostatic field strength of 15 kV/10 cm.

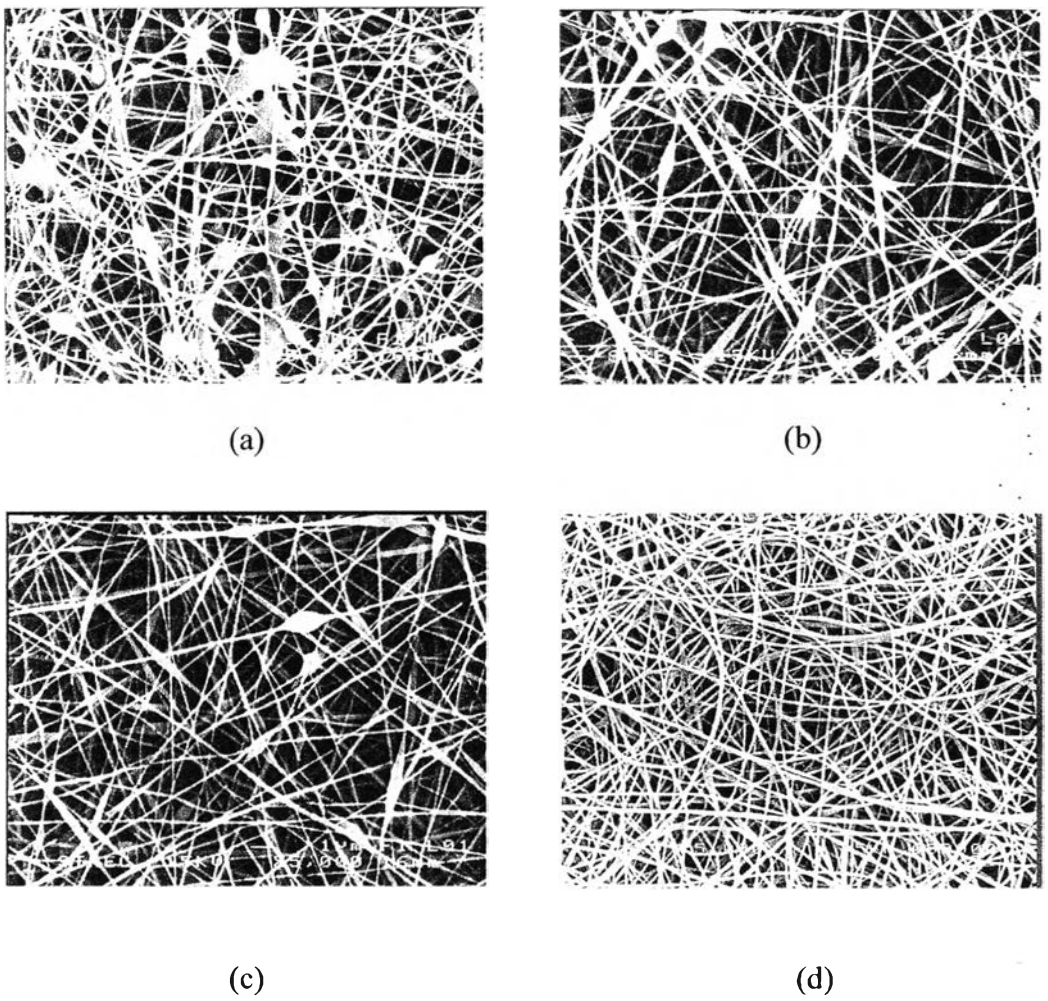

Figure 5.2 Selected scanning electron microscope images illustrating the morphological appearance of electrospun fibers from poly(vinyl alcohol) (10 wt%)/tin glycolate solution under 12.5 kV/15cm in various types of media of (a) H_2O, (b) 8M CH_3COOH, (c) 8M HCl, and (d) 8M HNO_3. The diameters of these fibers were 238 ± 153, 199 ± 97,177 ± 84, and 143 ± 23 nm, respectively.

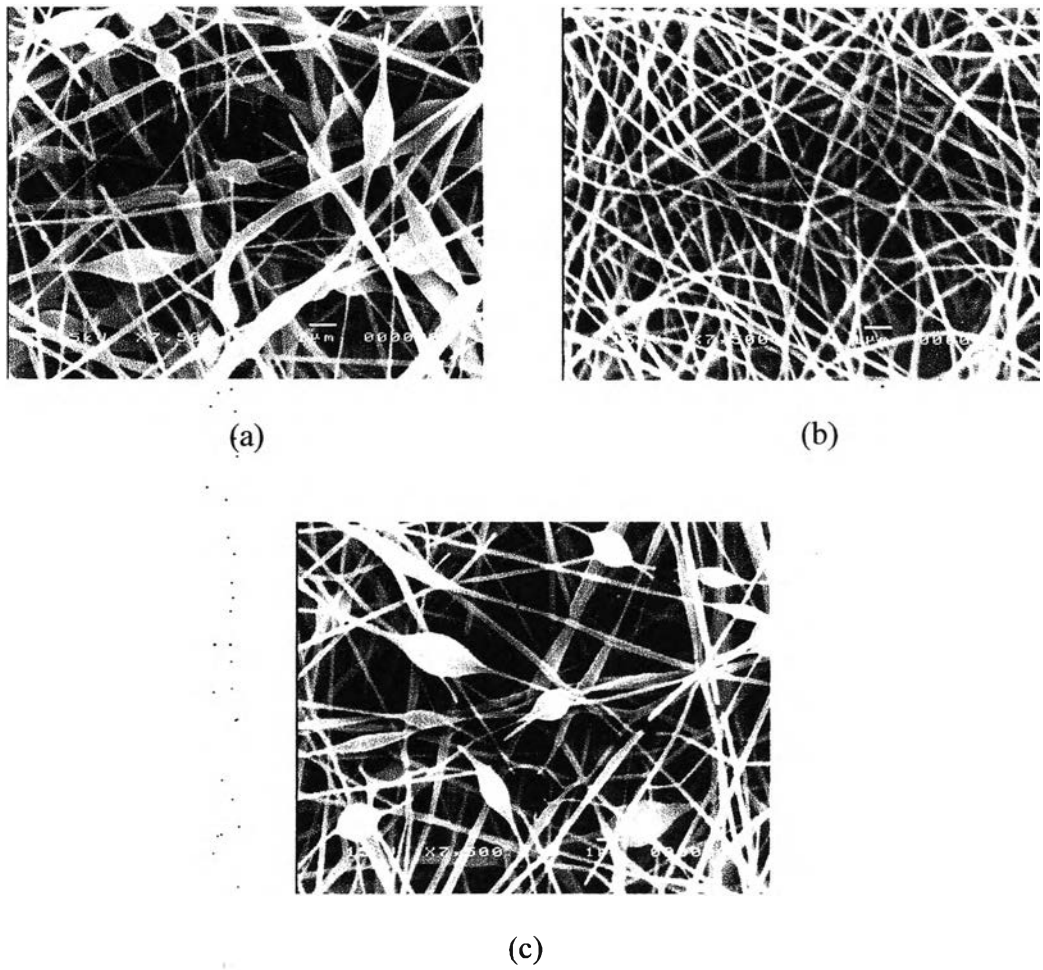

Figure 5.3 Selected scanning electron microscope images illustrating the morphological appearance of electrospun fibers from poly(vinyl alcohol) (10 wt%)/8M HNO_3/tin glycolate solution under the various electrical potentials of (a) 10, (b) 12.5, and (c) 15 kV that were applied over a fixed collection distance of 15 cm. The diameters of these fibers were 241 ± 104, 143 ± 23, and 194 ± 72 nm, respectively.

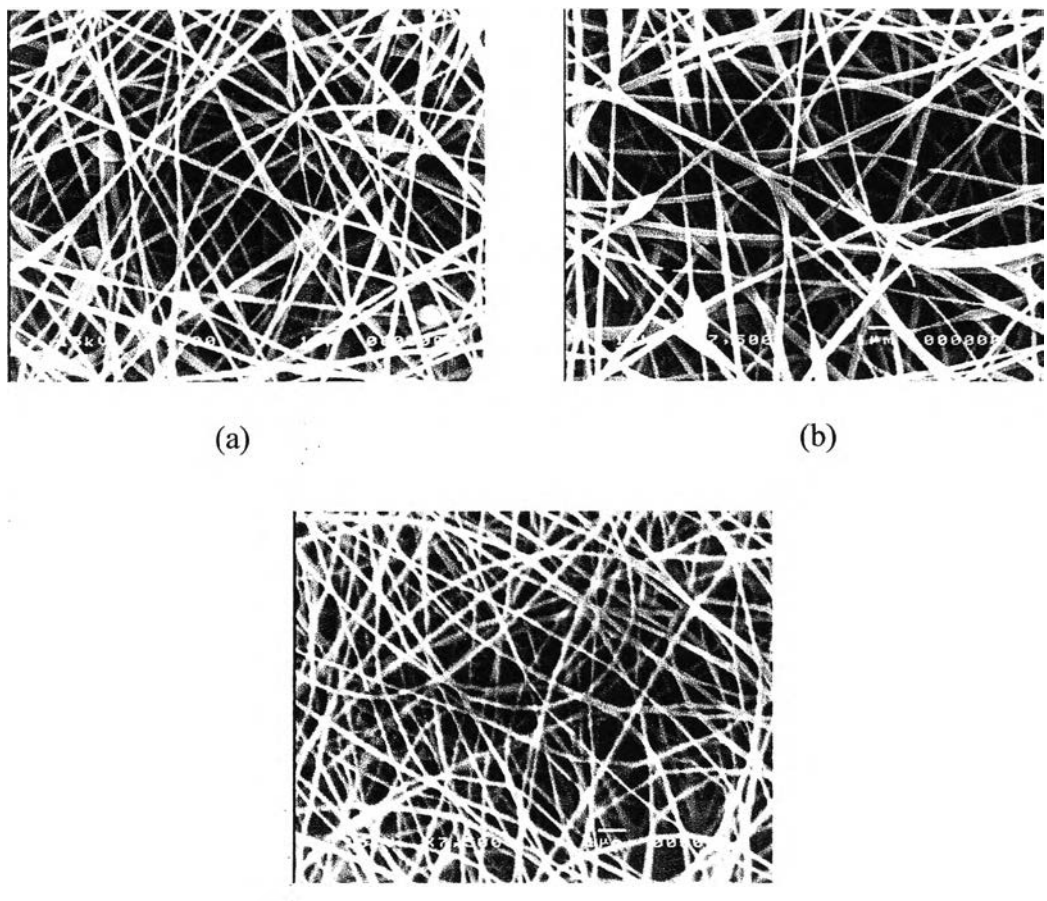

Figure 5.4 Selected scanning electron microscope images illustrating the morphological appearance of electrospun fibers from poly(vinyl alcohol) (10 wt%)/8M HNO_3/tin glycolate solution under a fixed applied electrical potential of 12.5 kV that was applied over various collection distance of (a) 8, (b) 10, and (c) 15 cm. The diameters of these fibers were 227 ± 85, 179 ± 45, and 147 ± 33 nm, respectively.

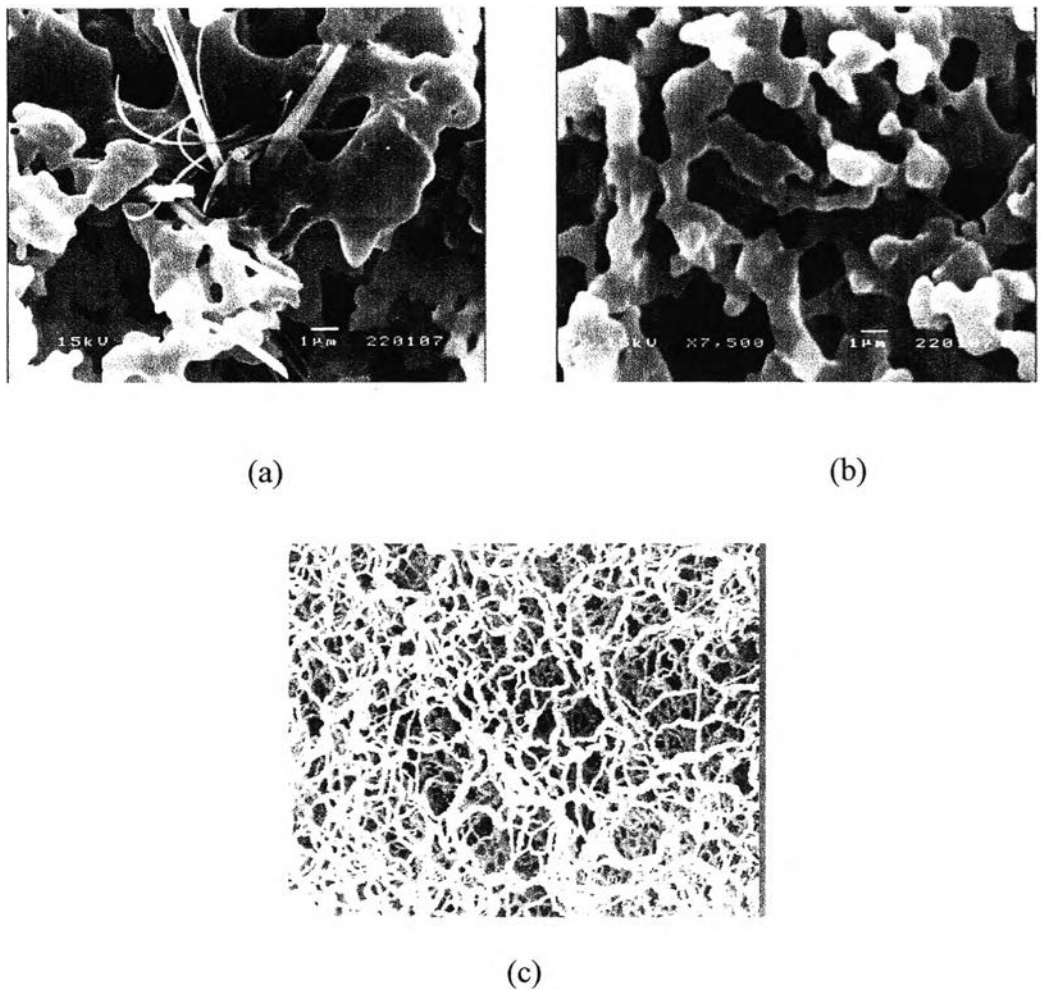

Figure 5.5 Selected scanning electron microscope images illustrating the morphological appearance of tin oxide fibers obtained from the calcinations at 600°C of electrospun poly(vinyl alcohol) (PVA)/tin glycolate composite fibers prepared from PVA (10 wt%)/tin glycolate solution under the applied electric field of 12.5 kV/15 cm at various type of acid (a) 8M CH_3COOH (b) 8M HCl, (c) 8M HNO_3, The diameters of these fibers were 1470 ± 88, 1249 ± 41, and 121 ± 126 nm, respectively.

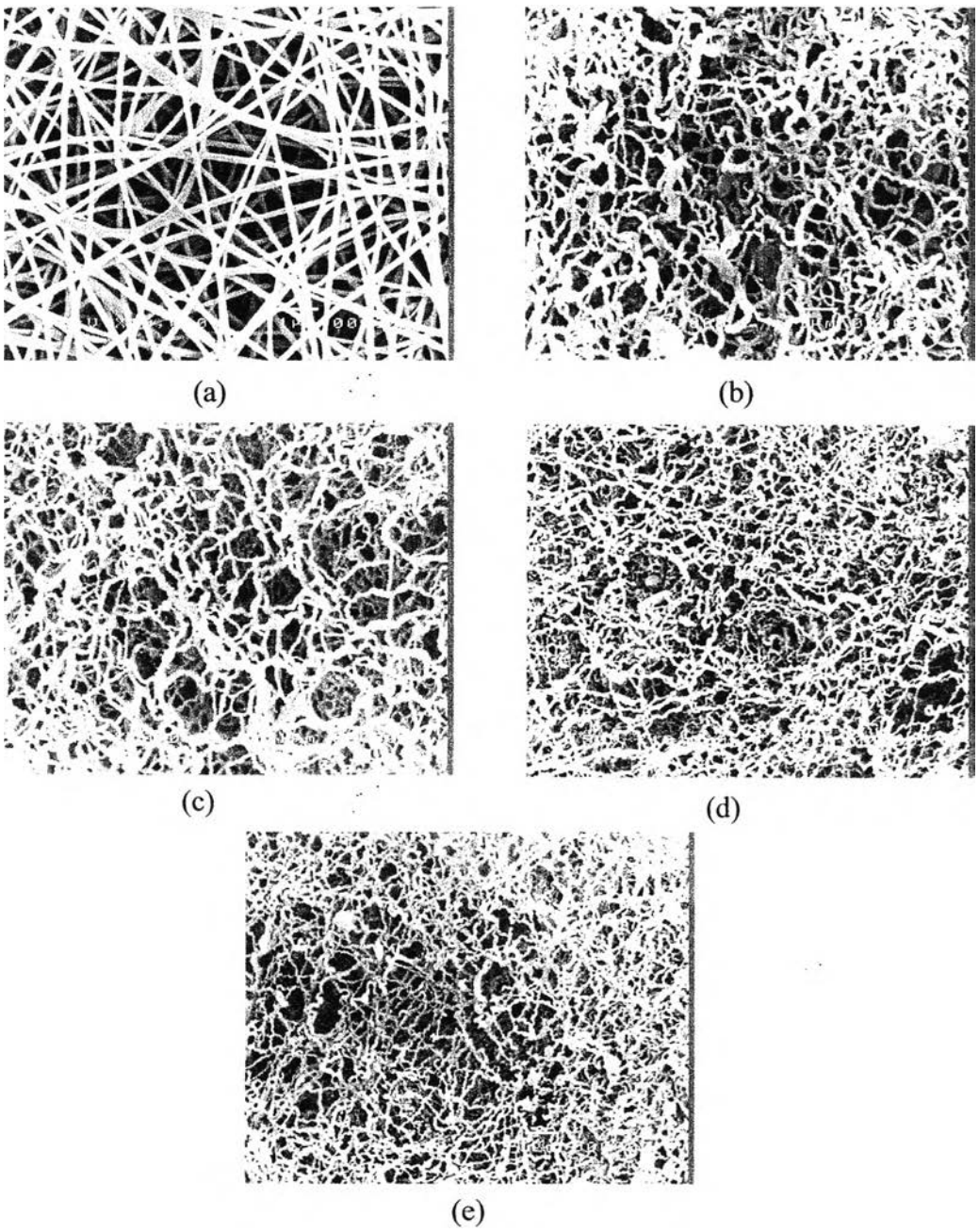

Figure 5.6 Selected scanning electron microscope images illustrating the morphological appearance of (a) precalcined electrospun poly(vinyl alcohol) (PVA)/tin glycolate composite fibers prepared from PVA (10 wt%)/8M HNO_3/tin glycolate solution under the applied electric field of 12.5 kV/15 cm and tin oxide fibers that were obtained from the calcination at various temperatures of (b) 400°C, (c) 600°C, (d) 800°C, and (e) 1000°C. The diameters of these fibers were 172 ± 21, 166 ± 46, 121 ± 26, 109 ± 24, and 87 ± 18 nm, respectively.

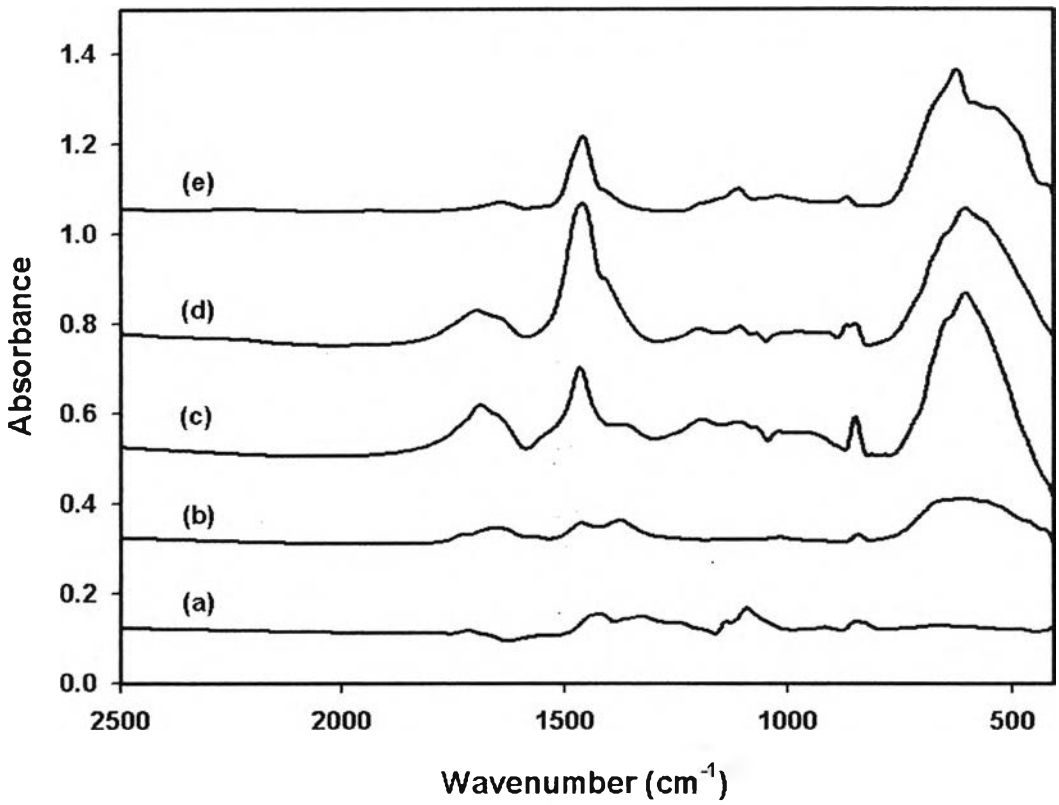

Figure 5.7 Fourier-transformed infrared spectroscopy spectra of (a) precalcined electrospun poly(vinyl alcohol) (PVA)/8M HNO_3/tin glycolate composite fibers prepared from PVA (10 wt%)/tin glycolate solution under the applied electric field of 12.5 kV/15 cm and tin fibers obtained from the calcinations at various temperatures of (b) 400°C, (c) 600°C, (d) 800°C, and (e) 1000°C.

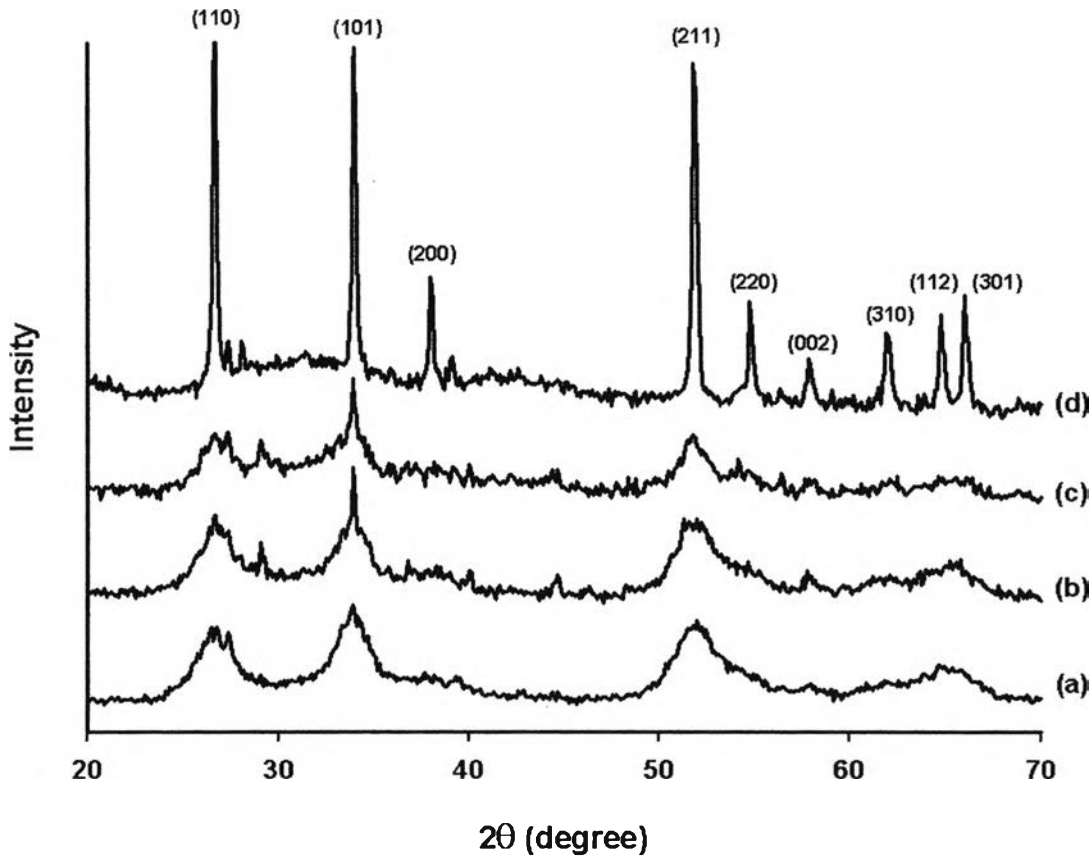

Figure 5.8 Wide-angle X-ray diffraction patterns of tin oxide fibers obtained from the calcination of electrospun poly(vinyl alcohol) (PVA)/tin glycolate composite fibers prepared from PVA (10 wt%)/8M HNO_3/tin glycolate solution under the applied electric field of 12.5 kV/15 cm at various temperatures of (a) 400°C, (b) 600°C, (c) 800°C, and (d) 1000°C.